Appl. Phys. B 52, 251–258 (1991)

Applied Physics B Photophysics and Laser Chemistry

Effect of Mechanical Tissue Properties on Thermal Damage in Skin After IR-Laser Ablation

M. Frenz[1], **Ch. Mischler**[2], **V. Romano**[1], **M. Forrer**[1], **O. M. Müller**[2], **and H. P. Weber**[1]

[1] Institute of Applied Physics and [2] Anatomical Institute, University of Berne, Sidlerstrasse 5, CH-3012 Berne, Switzerland

Received 19 October 1990/Accepted 10 December 1990

Abstract. The damage created instantaneously in dorsal skin and in the subjacent skeletal muscle layer after CO_2 and Er^{3+} laser incisions is histologically and ultrastructurally investigated. Light microscopical examinations show an up to three times larger damage zone in the subcutaneous layer of skeletal muscle than in the connective tissue above. The extent of thermally altered muscle tissue is classified by different zones and characterized by comparison to long time heating injuries. The unexpectedly large damage is a result of the change of elastic properties occurring abruptly at the transition between different materials. This leads to a discontinuity of the cutting dynamics that reduces the ejection of tissue material. We show that the degree of thermal damage originates from the amount of hot material that is not ejected out of the crater acting as a secondary heat source.

PACS: 61.80.Ba, 87.45.Bp, 87.69.Gp

Lasers, as medical tools, have widely been used for surgical, diagnostic and therapeutic applications [1–4]. Used in surgery, their main advantage compared with the mechanical scalpel is the instant generation of a coagulation zone along the incision walls which leads to haemostasis. To achieve a rapid healing and to avoid an undesirable large scar formation during the healing process, the width of tissue damage should be minimized [5]. The extent of the damage zone is not only a function of the laser parameters used, but also a function of the tissue type [6–9]. A considerable number of organs consist of various different tissue types superimposed onto each other. Examples are skin, the vocal cords, the stomach or thick vascular membranes. Surgeons want to cut them with the laser in a rapid and precise way.

The purpose of this investigation was first to study the influence of the mechanical tissue properties on the dynamics of the cutting process at the material boundaries between tissue types and second to determine and to characterize the extent of the created damage in each tissue layer. We compare the amount and type of damage in the connective tissue of the corium and in the subjacent muscle layer when cutting skin. A histological and ultrastructural comparison of the altered tissue to samples subjected to a controlled temperature treatment in a heat bath will then allow to differenciate between thermal and mechanical damage. Additional studies with a composite structure of the tissue substitutes gelatin and agar show time-resolved the dynamics of the hole formation at such a material boundary. The large extent of altered tissue in the muscle layer is then explained by heat dissipation of hot liquefied material trapped in the created cavity.

1. Materials and Methods

Our measurements were performed using either a flashlamp pumped free-running Er^{3+}:YAG laser emitting radiation at $\lambda = 2.94\,\mu m$ or a slow axial flow CO_2 laser producing pulses at $\lambda = 10.6\,\mu m$. Both lasers were operating in the TEM_∞ mode at a repetition rate of 4 Hz. The pulse duration was 200 µs for the erbium laser and between 100 µs and 1 ms for the CO_2 laser. The temporal power profile of the erbium laser was essentially rectangular up to a 10% variation of the peak intensity on a µs time scale. That one of the CO_2 laser was smooth and bell-shaped. The laser light was focused perpendicularly onto the surface of the samples. The spot size was determined by measuring burn patterns on a black anodized Al plate and using the calculation given in [6].

1.1 Laser Incisions in Tissue

All tissue experiments were performed on both, shaved dorsal skin of anesthetized male ICR albino mice (in-

tramuscular injection of a mixture of ketamine-xylazine-acepromazine) and gluteal muscle, excised immediately after sacrificing. The samples were mounted on a controllable x-y-table which allowed to make reproducible line cuts of 1 cm length. For that purpose identical laser pulses were focused side by side and between successive pulses the sample was shifted by the radius of the spotsize. To study the influence of the direction of the myofibriles in the skin muscle, the incisions in the dorsal skin were made in parallel and perpendicular direction to the spinal cord of the mouse. The laser intensity was adjusted in such a way that on the one hand the depth of the created cuts was deep enough to divide the skin muscle by each laser pulse, on the other hand the intensity was sufficiently low to avoid the appearance of the instabilities [6] in the drilling process. From previous studies [6] we specified the intensity to be less than $127\,J/cm^2$ for the Er^{3+} laser and less than $354\,J/cm^2$ in the case, where the longer wavelength of the CO_2 laser is used.

For histological investigations the laser-treated tissue samples were fixed in formalin immediately after irradiation, dehydrated in ethanol and embedded in paraplast. The sections were stained with Mallory-Azan and hematoxylin and eosin (H+E). Mallory-Azan allows to determine the thermally destroyed tissue by its red color, whereas the intact one appears blue [10]. The damaged tissue can be visualized by the loss of the naturally occurring birefringence of the collagen fibres [11].

For ultrastructural analyses in the electron microscope all samples were fixed in glutaraldehyde (3.125%) and osmium tetroxyde (1% in 0.1 M sodium-cacodylate/HCl-buffer, pH 7.4, 340 mOs mol), dehydrated in ethanol, embedded in Epon, cut into ultrathin sections, and stained with uranyl acetate and lead citrate.

1.2 Heat Bath Experiments

To estimate the temperatures arising during the laser impact and to prove whether the tissue alterations are exclusively due to thermal effects, we compared the laser injury to tissue samples thermally damaged by immersion in a heat bath of constant temperature for 160 s. This duration guaranteed that everywhere inside the sample the temperature had reached the value of the surrounding liquid. The experiment was carried out for temperatures of the heat bath ranging from 53 to 150° C, as described in detail in a previous publication [7]. For histological and ultrastructural investigations these samples were handled in the same way as after laser treatment.

1.3 Incisions into a "Tissue Model"

As a substitute for the layer structure of the skin we used a composite structure of agar, gelatin and agar. This composition has similar mechanical properties to skin. For a given water content gelatin has an elasticity comparable to muscle tissue, whereas agar, which is more rigid, corresponds to the connective tissue of the skin.

The optical transparency of the tissue substitutes enabled us to study the effect of radiation impact in a time-resolved way by means of high speed photography. Either single snapshots or series of up to 18 consecutive frames could be taken of a single event at repetition rates as high as 5×10^5/s. This allowed quick and accurate determination of the instantaneous shape and the depth of the drilled holes during the laser impact.

2. Results

2.1 Histological and Ultrastructural Evaluation after Laser Incision

The light microscopical examination of the incisions produced in the dorsal skin of anesthetized mice show great differences of the extension of lateral thermal damage along the edge of the craters between the different tissue layers, as shown in Fig. 1. Independently of the wavelength used, we distinguished in the corium two thermally altered zones; the coagulation zone and the transition zone, marked in Fig. 1a, b by 1 and 2, respectively. This distinction and the histological characterization of these zones have already been made in previous publications [3, 7]. The subcutaneous layer of skeletal muscle, however, shows an approximately threefold increase of the extent of damage (Fig. 1a, b). It is remarkable that the direction of the cut, whether parallel or perpendicular to the spinal cord of the mouse, has no influence on the instantaneously created lateral extension of the damage. This dramatic lateral extension of damaged muscular tissue can be classified light microscopically by different structural changes (compare zone I–V of Fig. 2).

Figure 2 shows a light microscopical and Fig. 3 an electron-microscopical view of the cross-section of the skin muscle after laser impact. The first zone (I), up to 50 µm thick, stains bright red after Mallory-Azan with a completely homogeneous appearance and a loss of the birefringence. Even electron-microscopically, no cellular details can be distinguished (Fig. 3a). The muscle fibers seem totally homogenized, no basement membranes can be identified. The quantification of the extent of this zone is difficult. First, because it does not always appear and moreover it is neither of uniform thickness nor symmetrically distributed along the walls of the laser crater. Carbonization as described by Viehberger et al. [12] using a 6–10 W cw CO_2 laser was not observed in the pulsed operation.The next zone (II), up to 250 µm thick, seems histologically to be composed of intact muscle cells but with a concentric lamination of the Z-bands (Fig. 3b). Nevertheless the high resolution of the electron microscopy indicates the totally dissolved mitochondria and severely destroyed nuclei. Zone III (150–200 µm thick) shows similarly to zone I ruptured, dark red stained muscle fibers. The ultrastructural comparison, however, revealed a different picture. The basement membrane is preserved and the mitochondria partly swollen but with intact outer membranes. The cells of the adjacent zone IV, the zone of the largest extension (up to 1300 µm thick) show a similar appearance. The actin and myosin filaments are partially visible resulting in the normal cross striation. The muscle cells of zone (V), furthest from the cutting edge seem to be unchanged under light microscopical resolution. In

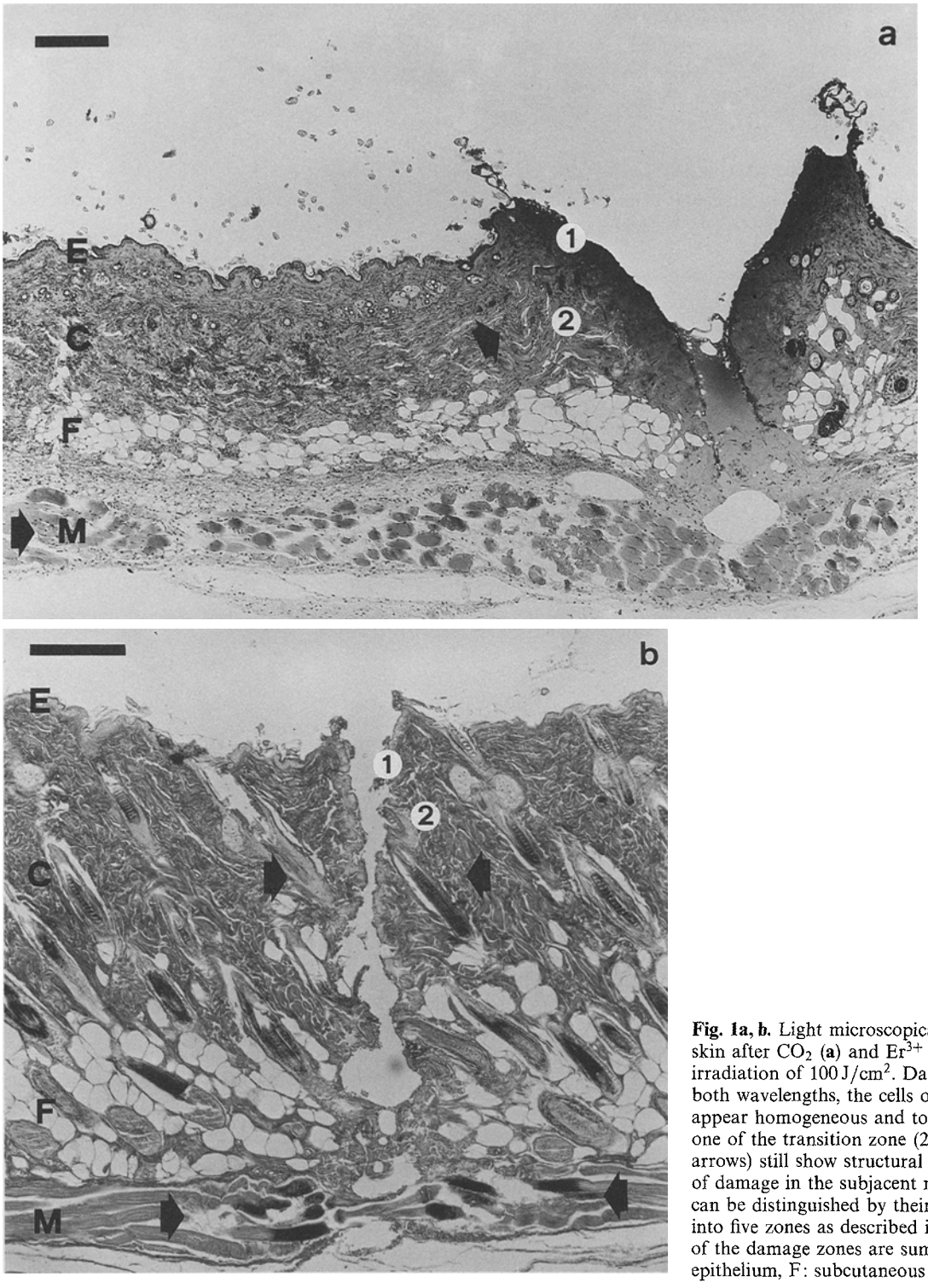

Fig. 1a, b. Light microscopical appearance of dorsal skin after CO_2 (**a**) and Er^{3+} (**b**) laser incisions with an irradiation of 100 J/cm^2. Damage of the corium C: for both wavelengths, the cells of the coagulation zone (1) appear homogeneous and totally dissolved, while this one of the transition zone (2) (extension marked by arrows) still show structural details. The large extent of damage in the subjacent muscle layer M (arrows) can be distinguished by their structural appearance into five zones as described in the text. The widths of the damage zones are summarized in Table 1 (E: epithelium, F: subcutaneous fat layer, bar = 200 µm)

contrast to that, the ultrastructure of these cells reveals a diminished periodicity of the sarcomere and the partly swollen mitochondria. Using the Er^{3+} laser for cutting, qualitatively the same distinction of the muscle damage into five zones can be done, quantitatively, however, the total thickness of the altered zone is, because of the ten times lower optical penetration depth of the Er^{3+} laser [13, 14] much thinner [15] (compare Fig. 1b). The results for the lateral extensions of the thermally damaged zones along the laser incisions in skin are summarized for both wavelengths in Table 1.

To demonstrate the influence of the structure in the composition of skin on the extent of the lateral damage we repeated the laser incisions in either connective tissue or muscle tissue, exclusively. Opposite to the corium (70% water content), the skeletal muscle (80% water content)

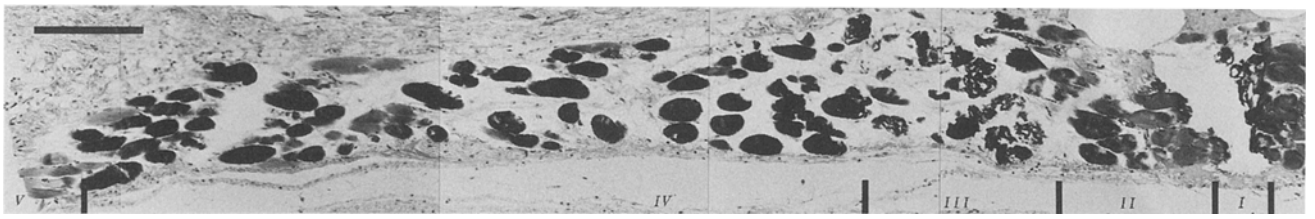

Fig. 2. Photomicrograph of the subcutaneous muscle layer after Co_2 laser treatment. Five zones of different cellular damage can be distinguished. Zone I means the area adjacent to the crater edge (Bar: 200 μm)

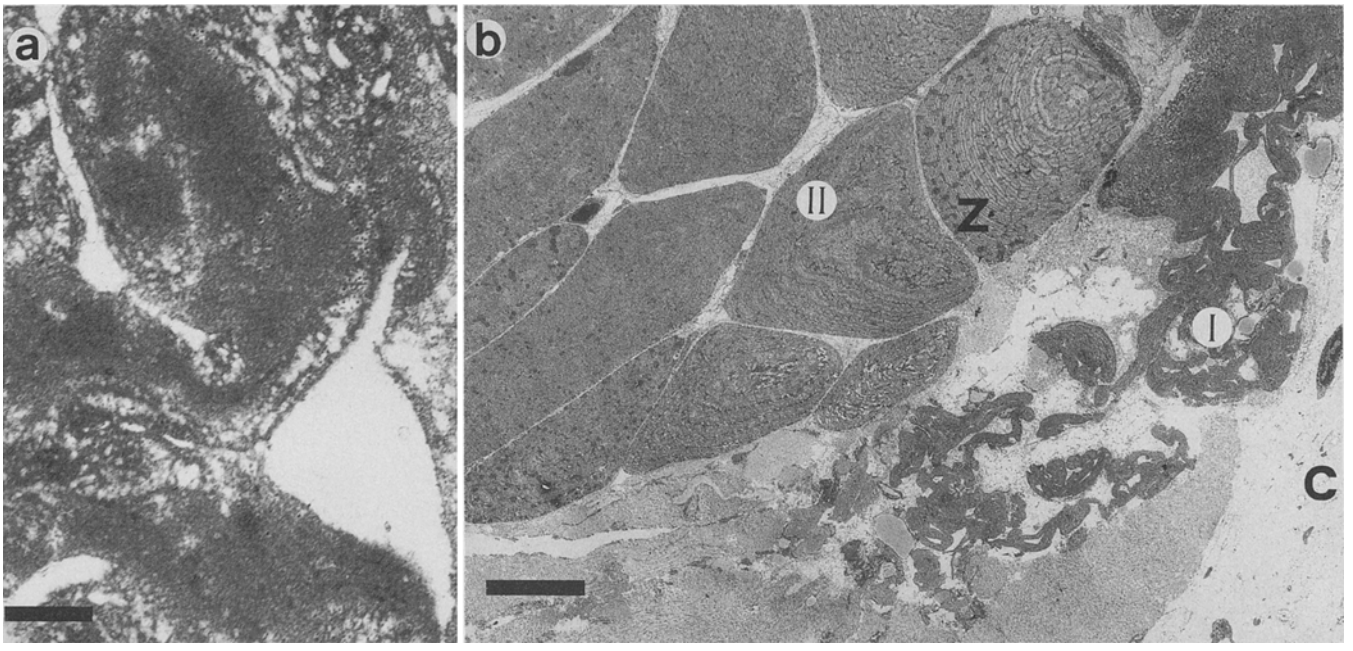

Fig. 3a, b. Transmission electron micrograph of the transversal section of the crater edge after Er^{3+} laser impact. **a** Closeup of zone I of Fig. 2. It shows the existence of a large number of vacuoles, besides no structural details can be distinguished (Bar = 0.5 μm). **b** Closeup of the boarder between zone I and zone II of Fig. 2. The helical structure of the Z-bands is clearly seen in zone II (Bar = 10 μm, C: crater)

represents a tissue with a high elasticity. The experiments were performed with the Er^{3+} laser at two intensities, 120 and 226 J/cm^2, a value below and far above the threshold of the appearance of mechanical instabilities, respectively.

As shown in [16], such instabilities occur during the drilling process in isotropic media for high laser intensities. They reduce the ejection of liquefied tissue out of the hole. The trapped hot liquid then acts as a heat reservoir and transfers the heat to the walls of the ablation crater, thereby bringing more of the surrounding tissue into the temperature range of coagulation. The extent of thermal damage in pork skin and gluteal mouse muscle for both laser irradiances is summarized in Table 2. Even for the high irradiance of 226 J/cm^2 the width of the damage zone in muscle amounts at most to only 220 ± 60 μm, about half of that if the muscle is embedded between connective tissue.

Table 1. Extension of the histologically determined zone of thermal damage after laser incision

	Er^{3+} Incision	CO_2 Incision
Corium		
Coagulation zone	42 ± 3 μm	102 ± 16 μm
Transition region	125 ± 50 μm	375 ± 52 μm
Skin muscle		
Damage zone I-IV	432 ± 365 μm	1800 ± 200 μm

Fig. 4a–f. Transmission electron micrographs of longitudinal sections of mouse muscle. The samples were thermally altered by immersion in a heat bath of temperature T for 160 s (Bar = 0.5 μm). **a** T = 20° C: completely intact appearance. The sarcomere, the area between two Z-bands (Z), is composed of a light (isotropic) zone, the I-band (I), and a dark (anisotropic) zone, the A-band (A), bisected by the M line. The dark and light regions represent the thick (myosin) and thin (actin) filaments, respectively [17] (T: Triad, part of the tubular system). **b** T = 53° C: The sarcomere length is reduced to about two-third of the normal length. The Z-bands have disappeared, the triads (T) are recognizable but swollen. **c** T = 65° C: The Z-bands are visible again, the mitochondria damaged. **d** T = 73° C: similar to **c**, but a frequently clumping of the cytoplasma is observed. The protein is contracted and coagulated. **e** T = 88–124° C: The proteins in the region of the Z- and I-bands are heavily condensed, the tubular system and the mitochondria are totally destroyed and appear dense in the electron microscope. **f** T = 150° C: No cellular details can be distinguished, the muscle seems to be homogenized showing a large number of vacuoles

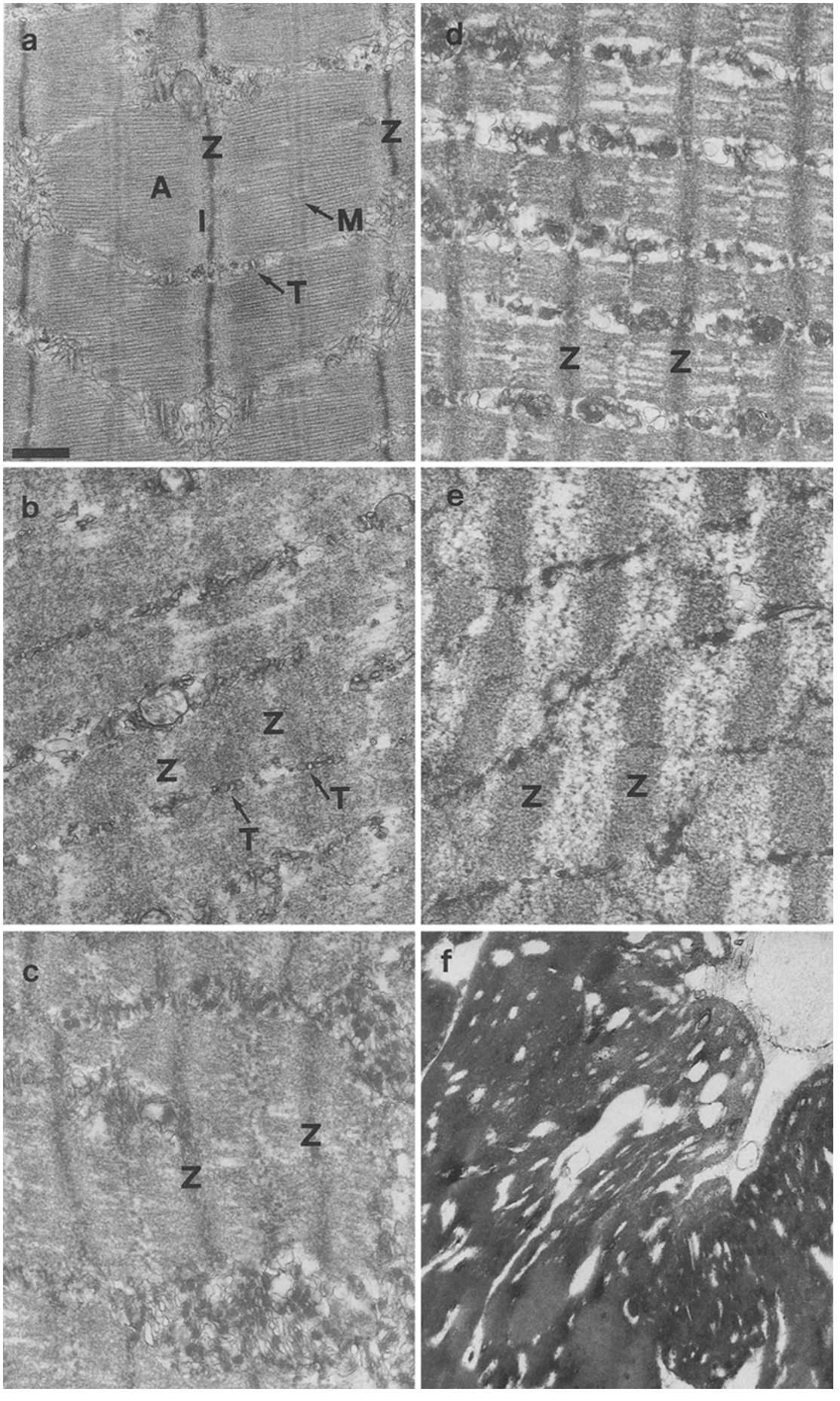
a
Z
Z
A
I
M
T
d
Z
Z
b
Z
Z
T
T
e
Z
Z
c
Z
Z
f

2.2 Comparison with Findings from the Heat Bath

The comparison on the light microscopical level discloses two points of interest. (i) If the samples were heated up to 65° C the muscle cells show an intact appearance as seen in zone V. On the other hand the epithelium is already completely, the collagen partially coagulated [7]. This corresponds to a damage situation found in the transition region of the corium after laser treatment. From the light microscopical point of view the thermal susceptibility of muscle seems to be lower than the one of corium. (ii) Heated up to temperatures of 150° C the muscle cells show no comparable structure like the one of zone III. Consequently, the ruptured structure cannot be damage-induced by temperature but seems to be of mechanical origin.

The ultrastructural examination of the samples after treatment in the heat bath gives a more detailed picture of the structural damage.

At 20° C the skeletal muscle shows a normal appearance (Fig. 4a). The two main protein components are myosin (length = 1.5 µm, Φ = 10 nm) and actin (length = 1 µm, Φ = 5 nm). The actin filaments are fixed at the Z-bands forming the I-band. The myosin is the major component of the A-band, attached to the M-line. The length of the sarcomere (the distance between two Z-bands) which represents the basic contractile unit is about 1.6 µm.

At 53° C the Z-bands have disappeared and the sarcomere is contracted. The triad seem to be completely intact.

At 65° C the Z-bands can again be detected. The membranes of the tubular system are still recognizable, the mitochondria heavily swollen. As mentioned above this muscle tissue seems light-microscopically intact (compare zone V).

At 73° C the sarcomere are contracted, actin and myosin are shrunk after coagulation. The mitochondria are damaged.

Between 88–124° C the muscle cells have lost their original structure and became "heat-fixed". Therefore their thermal alterations remain constant. The damage picture cannot be distinguished from the one of zone II, except for the concentric lamination of the Z-bands, not observed after treatment in the heat bath.

At 150° C the muscle cells are completely homogenized without any appearance of a cellular structure. Figure 4f shows the same ultrastructural appearance as observed in zone I (compare Fig. 3a).

2.3 The Tissue Model

If one drills holes into targets that are homogeneous from the mechanical point of view and if the intensity of the drilling laser pulse is kept below 127 J/cm^2 to avoid the appearance of the instabilities [6, 16], the hole diameter does not show any major variations along the axis of the drilled craters. This is no longer the case, however, when drilling through a transition between two materials with different elasticities. At the material boundary inside the target the hole "blows up" (Fig. 5) to a diameter that shows a more than threefold enhancement compared to the one observed in homogeneous targets of the respective material (compare the diameter at the positions 1 and 2). Even for laser intensities far above the threshold for the appearance of the instabilities, the hole diameter at the material boundary is still twice as large as the one

Fig. 5. The shape of the laser drilled hole in an agar-gelatin target at the end of the laser pulse. The hole diameter at the position 1 indicates the normal diameter drilling into the rigid agar material. Just below the material boundary the diameter increases up to more than 3 times than the one 1 mm below (position 2). (CO_2 laser: 300 J/cm^2, τ = 400 µs)

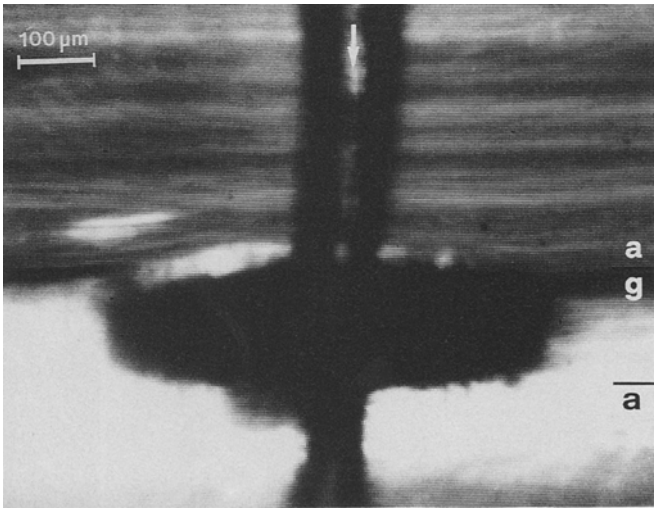

Fig. 6. The picture shows the shape of the hole at the end of the CO_2 laser pulse drilled into the composite structure of an agar-gelatin-agar target used to simulate the layer structure of skin. Inside the gelatin layer the hole diameter is about five times larger than in the agar material. (CO_2 laser: 300 J/cm^2, τ = 400 µs)

induced by the instabilities. Figure 5 displays a snapshot of the shape of the hole just at the end of a 400 µs long CO_2 laser drilling pulse at a fluence of 300 J/cm^2. The target material was a structure with a transition from agar to gelatin.

The complete sandwich structure of the skin was modeled by a target composed of a 150 µm thick gelatin layer embedded between two agar samples. The dramatic deformation of the hole diameter at the material boundaries when drilling through this composite structure is illustrated in Fig. 6.

Table 2. Effect of laser irradiance on tissue damage in skin and skeletal muscle

	120 J/cm^2	226 J/cm^2
Skeletal muscle		
Damage zone I–IV	45 ± 8 µm	220 ± 60 µm
Drilling depth	2.8 mm	5.3 mm
Connective tissue		
Coagulation zone	55 ± 6 µm	150 ± 60 µm
Drilling depth	2.1 mm	3.6 mm

3. Discussion

The results of this study show that, when cutting skin up to a depth where the skin muscle gets divided, the lateral extent of the thermal damage produced in corium differs substantially from the one in muscle tissue. The up to three times larger width of altered tissue in the subcutaneous layer of skeletal muscle (compare Table 1) can, however, not be explained by a higher thermal susceptibility of the muscle cells as stated by Ben-Basset et al. [18]. Comparison of the thermal damage after treatment in a heat bath reveals that from the light microscopical point of view, used for the characterization of the damage, the muscle seems to be even less sensitive. This is further emphasized by the lower tissue damage in the homogeneous tissue of skeletal muscle after laser impact with an irradiance of 120 J/cm^2 (Table 2).

It is generally accepted that the mechanical forces caused by the recoil-pressure of the evaporated molecules play an important role in the ablation process of soft tissue. They lead at the phase boundary to a radial displacement of liquefied material out of the irradiated region and to an expulsion out of the hole. Depending on their strength and the elastic properties of the material the diameter of the created crater increases up to several times the size of the beam diameter [6]. The softer the material the more this becomes pronounced, leading to a higher efficiency of the drilling process. This is confirmed by the deeper drilling depht in the soft skeletal muscle compared to that in the more rigid connective tissue (Table 2).

For the high laser irradiance of 226 J/cm^2 the drilling process is in the regime where mechanical instabilities take place. They are visualized by strong spatial variations of the hole diameter which are more pronounced the higher the elasticity and the lower the viscosity of the target material [6]. As a result, the hot liquefied tissue material remains trapped in these cavities and represents the essential second heat source of the damage [7, 16, 19]. Thus the dramatical increase of the damage created in the muscle tissue by the high Er^{3+} laser irradiance is due to its soft mechanical material properties.

The shape of the hole drilled into the composite structure consisting of agar and gelatin (Figs. 5 and 6) shows at the material boundary a similar, but even more pronounced spatial variation of the hole diameter. When filled with hot liquefied tissue, this large cavity represents an efficient heat reservoir. The heat diffusion from this large amount of hot liquefied tissue is not only the reason for the extended damage of the skeletal muscle, but influences also the surrounding tissue. The maximal value of the extent of thermally altered connective tissue in the corium is found right above the subcutaneous fat layer. The appearance of the dramatic increase of the hole diameter at the material boundary occurs even at laser intensities, where no instabilities are observed in the homogeneous material.

If the laser beam penetrates the material boundary from the rigid to the soft material, the hole diameter rapidly becomes enlarged. In the soft material the drilling velocity increases as mentioned above. This enhances the axial upward flow of liquefied material. Because of the narrowness of the hole in the upper layer, part of the liquid continuously splashes back into the laser beam. This locally rises the evaporation rate and the pressure inside the hole with a resulting additional increase of the hole diameter. The geometrical situation of this process is illustrated in Fig. 7. The findings of the high-speed photography confirm this fact. It reveals that the hole in the soft layer continuously increases during the duration of the pulse. In contrast, the enhanced diameter of the hole caused by the instabilities at the phase boundary remains constant during the laser pulse [16].

The evaporation of liquefied material rejected into the laser beam consumes a considerable part of the incident laser energy. Thus the drilling velocity in the lower agar layer is only about half of the one in the upper layer, although the temporal pulse profile is almost rectangular. This attenuation of the laser beam reduces the final drilling depth. Actually, the measured drilling depth in skin, if drilled through the skin muscle, is only 1.5–1.7 mm compared to a crater depth of 2.0–2.2 mm in the homogeneous corium (Table 2).

The ablation process and its dynamics give some guidance for interpreting the damage structures of the different zones in the muscle tissue. The cells of zone I, totally homogenized, might have been heated up to at least 150° C. The thermally altered tissue shows the same electron microscopical appearance as the one heated up to 150° C in the heat bath. Because of the high pressure at the material boundary, the muscle layer is mechanically strongly compressed during the laser pulse. Up to a distance where the induced temperature is sufficiently high the tissue becomes heat fixed under the existing conditions. If contracted fixed muscle bundles are laterally sectioned the picture shows the helical structures observed in zone II. From measurements in gelatin it is known that during the laser pulse the hole diameter is

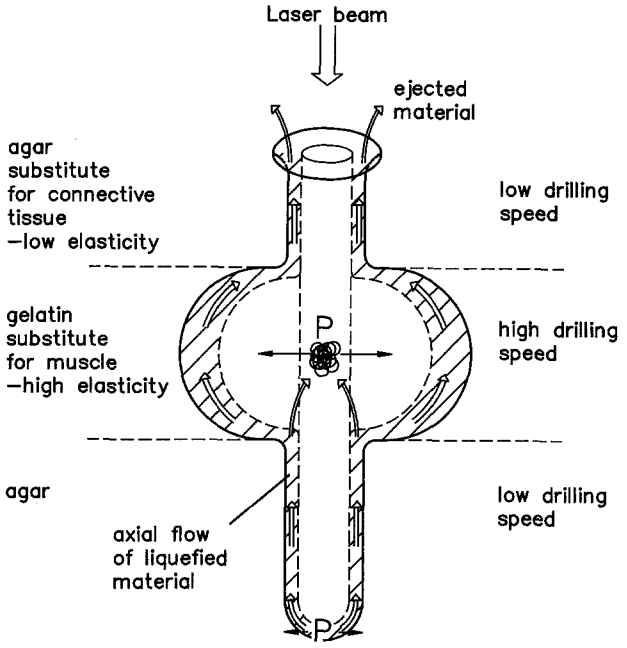

Fig. 7. Schematic illustration of the dynamic of the ablation process at the material boundary

substantially larger than the beam diameter. Afterwards it shrinks elastically. After the heat fixation, the muscle bundles become rigid and lose their elasticity. Therefore the adjacent thermally damaged bundles are torn apart during the relaxation process. This explains the damage structure of zone III, only observed in the embedded muscle layer after laser impact.

4. Conclusions

The sequence of histological changes induced by intense infrared laser irradiation was discussed in terms of the elastic material properties of the tissue and the dynamics of the drilling process. The damage structures of the areas adjacent to the crater after laser impact were compared to injuries induced by long-time heating. The differences are shown to be of mechanical nature. When drilling through a composite structure consisting of skeletal muscle and connective tissue an unexpectedly large extension of damage is created in the muscle layer. The large extension was found to be independent of the employed laser wavelength. Influenced by the high elasticity of the muscle tissue layer, the hole blows up, intensified by the pressure rise due to additional evaporation of liquefied tissue rejected into the laser beam. This renders the drilling of deep holes with a single exposure inefficient. Further hot liquefied tissue material trapped in the cavity represents the essential heat source.

The wide damage in the soft muscle layer and the resulting delayed wound healing must be taken into consideration if the laser is to be used in a region where tissue of different mechanical properties is affected and the cut is done with single laser exposures.

In order to minimize the thermal damage in the connective tissue as well as in the subcutaneous muscle layer care should be taken when drilling through a composition consisting of various tissue types with strongly different elastic properties. This can be achieved by performing the laser cut with successive pulses of short duration and low energy. Then the amount of liquefied tissue becomes small and most of it is ejected out of the hole.

Acknowledgements. The authors thank A. Friedrich for technical assistance and B. Krieger for preparation of the figures. This work was supported by the Swiss Science Foundation.

References

1. I. Kaplan: In: *Lasers in Biology and Medicine*, ed. by F. Hillenkamp, R. Pratesi, C.A. Sacchi (Plenum, New York 1980) pp. 347–351
2. R. Kaufmann, R. Hibst: Pulsed Er:YAG- and 308 nm UV-excimer laser: an in vitro and in vivo study of skin-ablation effects. Lasers Surg. Med. **9**, 132–140 (1989)
3. R.J. Lanzafame, O. Naim, D.W. Rogers, J.R. Hinshaw: Comparison of continuous-wave, choped-wave, and super pulse laser wounds. Lasers Surg. Med. **8**, 119–124 (1988)
4. L.I. Deckelbaum, M.L. Stetz, J.K. Lam, K.S. Clubb, F. Cutruccola, H.S. Cabin, M.V. Long: Fiberoptic laser induced fluorescence detection of artherosclerosis and plaque ablation; potential for laser angioplasty guidance. Circulation **74**(2), 27 (1986)
5. R.R. Hall: The healing of tissue incised by a carbon-dioxide laser. Br. J. Surg. **58**, 222–225 (1971)
6. M. Frenz, V. Romano, A.D. Zweig, H.P. Weber, N.I. Chapliev, A.V. Silenoc: Instabilities in laser cutting of soft media. J. Appl. Phys. **66**, 4496–4503 (1989)
7. A.D. Zweig, B. Meierhofer, O.M. Müller, Ch. Mischler, V. Romano, M. Frenz, H.P. Weber. Lateral thermal damage along pulsed laser incisions. Lasers Surg. Med. **10**, 262–274 (1990)
8. J.T. Walsh, T.J. Flotte, R.R. Anderson, T.F. Deutsch: Pulsed CO_2 laser tissue ablation: effects of tissue type and pulse duration on thermal damage. Lasers Surg. Med. **8**, 108–118 (1988)
9. J.T. Walsh, T.J. Flotte, T.F. Deutsch: Er:YAG laser ablation of tissue: effect of pulse duration and tissue type on thermal damage. Lasers Surg. Med. **9**, 314–326 (1989)
10. B. Romeis: *Mikroskopische Technik* (Oldenbourg, München 1968) p. 368
11. S. Thomson, J.A. Pearce, W. Cheong: Changes in birefringence as markers of thermal damage in tissues. IEEE Trans. BE-**36**, 1174–1179 (1989)
12. G. Viehberger, R. Fischer, P. Kyrle, H. Plenk: Ultrastructure of skeletal muscle after CO_2-laser incision. Res. Exp. Med. (Berl.) **176**, 69–79 (1979)
13. V.M. Zolotarev, B.A. Mikhailov, L.I. Alperovich, S.I. Popov: Dispersion and absorption of liquid water in the infrared and radio regions of the spectrum. Opt. Spectrosc. **26**, 430–432 (1969)
14. J. Frauchiger, W. Lüthy: Interaction of 3 μm radiation with matter. Opt. Quant. Electron **19**, 231–235 (1987)
15. A.D. Zweig, M. Frenz, V. Romano, H.P. Weber: A comparative study of laser tissue interaction at 2.94 μm and 10.6 μm. Appl. Phys. B **47**, 259–265 (1988)
16. M. Frenz, A.D. Zweig, V. Romano, H.P. Weber, N.I. Chapliev, A.V. Silenoc: Dynamics in laser cutting of soft media. In: *Laser-Tissue Interaction.* Proc. SPIE **1202**, 22–33 (1990)
17. H.E. Huxley: *The Structure and Function of Muscle*, ed. by G.H. Bourne, 2nd edn. (Academic, New York 1972) Vol. 1, pp. 302–387
18. Mi. Ben-Bassat, Mo. Ben-Bassat, I. Kaplan: A study of the ultrastructural features of the cut margin of skin and mucous membrane specimens excised by carbon dioxide laser. J. Surg. Res. **21**, 77–84 (1976)
19. K.T. Schomacker, J.T. Walsh, T.J. Flotte, T.F. Deutsch: Thermal damage produced by high-irradiance continuous wave CO_2 laser cutting of tissue. Lasers Surg. Med. **10**, 74–84 (1990)